

Simultaneous cooling of coupled mechanical resonators in cavity optomechanicsDeng-Gao Lai,¹ Fen Zou,¹ Bang-Pin Hou,² Yun-Feng Xiao,³ and Jie-Qiao Liao^{1,*}¹*Key Laboratory of Low-Dimensional Quantum Structures and Quantum Control of Ministry of Education, Department of Physics and Synergetic Innovation Center for Quantum Effects and Applications, Hunan Normal University, Changsha 410081, China*²*College of Physics and Electronic Engineering, Institute of Solid State Physics, Sichuan Normal University, Chengdu 610068, China*³*State Key Laboratory for Mesoscopic Physics and School of Physics, Peking University, Collaborative Innovation Center of Quantum Matter, Beijing 100871, China*

(Received 17 April 2018; published 30 August 2018)

Quantum manipulation of coupled mechanical resonators has become an important research topic in optomechanics because these systems can be used to study the quantum coherence effects involving multiple mechanical modes. A prerequisite for observing macroscopic mechanical coherence is to cool the mechanical resonators to their ground state. Here we propose a theoretical scheme to cool two coupled mechanical resonators by introducing an optomechanical interface. The final mean phonon numbers in the two mechanical resonators are calculated exactly and the results show that the ground-state cooling is achievable in the resolved-sideband regime and under the optimal driving. By adiabatically eliminating the cavity field in the large-decay regime, we obtain analytical results of the cooling limits, which show the smallest achievable phonon numbers and the parameter conditions under which the optimal cooling is achieved. Finally, the scheme is extended to the cooling of a chain of coupled mechanical resonators.

DOI: [10.1103/PhysRevA.98.023860](https://doi.org/10.1103/PhysRevA.98.023860)**I. INTRODUCTION**

The radiation-pressure coupling between electromagnetic fields and mechanical oscillation is at the heart of cavity optomechanics [1–3]. This coupling is the basis for both the control of the mechanical properties through the optical means and the manipulation of the field statistics by mechanically changing the cavity boundary [4–12]. In recent years, much attention has been paid to optomechanical systems involving multiple mechanical resonators [13–18]. This is because the multimode mechanical systems can be used to study macroscopic mechanical coherence such as quantum entanglement [19–26] and quantum synchronization [27,28]. Moreover, coupled mechanical systems have been widely applied to sensors for detecting various physical signals [29,30], especially in nanomechanical systems [29–33].

To observe the signature of quantum effects in mechanical systems, a prerequisite might be the cooling of the systems to their ground states such that the thermal noise can be suppressed. So far, several physical mechanisms such as feedback cooling [34–38], backaction cooling [39,40], and sideband cooling [41–49] have been proposed to cool a single mechanical resonator in optomechanics. Moreover, various schemes have been proposed to cool mechanical resonators, such as transient cooling [50,51], cooling based on the quantum interference effect [52–55], and quantum cooling in the strong-optomechanical-coupling regime [56,57]. In particular, the ground-state cooling has been realized in typical optomechanical systems, which is composed of a single cavity mode and a single mechanical mode [58,59]. Correspondingly, to

manipulate the quantum coherence in multimode optomechanical systems, it is desired to cool these mechanical modes for further quantum manipulation [60–62]. Nevertheless, how to cool multiple mechanical resonators remains an unresolved question.

In this paper, we present a practical scheme to cool two coupled mechanical resonators in an optomechanical system which is formed by an optomechanical cavity coupled to another mechanical resonator. Here, the two mechanical resonators are coupled to each other through the so-called position-position coupling, which can be physically realized either by using a piezoelectric transducer in paired GaAs-based mechanical resonators [31] or by introducing an electrostatic force between the two resonators [32,33,63,64]. In the strong-driving regime, the system is linearized to a three-mode cascade system, which is composed of a cavity mode and two mechanical modes. To include the cooling channel and the environments, we assume that the cavity field is connected with a vacuum bath, and the two mechanical resonators are connected with two heat baths at finite temperatures. Physically, the vacuum bath of the cavity field extracts the thermal excitations in the mechanical resonators via a manner of nonequilibrium dynamics, and then the total system reaches a steady state. By exactly calculating the final mean phonon numbers in the resonators, we find that the ground-state cooling of the two mechanical resonators can be realized simultaneously under the optimal driving detuning and in the resolved-sideband regime. Specifically, the cooling limits of the two mechanical resonators are analytically derived by adiabatically eliminating the cavity field in the large-decay regime. Finally, we extend the optomechanical scheme to the cooling of a chain of coupled mechanical resonators. The results show that ground-state cooling is achievable in multiple mechanical resonators,

*jqiao@hunnu.edu.cn

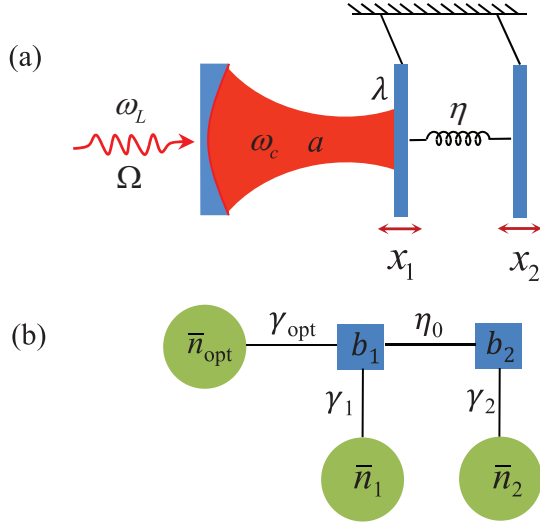


FIG. 1. (a) Schematic of the three-mode optomechanical system. A single-mode cavity field with resonance frequency ω_c is coupled to an oscillating end mirror with resonance frequency $\tilde{\omega}_1$ via the radiation-pressure coupling. The movable end mirror is coupled to another mechanical resonator with resonance frequency $\tilde{\omega}_2$ via the “position-position” interaction. (b) By adiabatically eliminating the cavity mode, the model in (a) is simplified to a system of two coupled mechanical modes b_1 and b_2 , with the coupling strength η_0 . The mechanical resonator $b_{l=1,2}$ is coupled to the heat bath with the decay rate γ_l and thermal occupation number \bar{n}_l . Additionally, the mode b_1 is coupled to an effective optical bath with the effective decay rate γ_{opt} and thermal occupation number \bar{n}_{opt} .

and that the cooling efficiency is higher for the mechanical oscillator, which is closer to the cavity.

The rest of this paper is organized as follows. In Sec. II, we introduce the physical model and present the Hamiltonians. In Sec. III, we derive the equations of motion and find the solutions. In Sec. IV, we calculate the final mean phonon numbers, analyze the parameter dependence, and derive the cooling limits of the two mechanical resonators. In Sec. V, we extend our studies to the case of a chain of coupled mechanical resonators. Finally, we present some discussions and a brief conclusion in Sec. VI. Two appendices are presented to display the detailed calculations of the final mean phonon numbers and the cooling limits.

II. MODEL AND HAMILTONIAN

We consider a three-mode optomechanical system, which is composed of one cavity mode and two mechanical modes, as illustrated in Fig. 1(a). The cavity-field mode is coupled to the first mechanical mode via the radiation-pressure coupling, and the two mechanical modes are coupled to each other via the so-called position-position interaction. To manipulate the optical and mechanical degrees of freedom, a proper driving field is applied to the optical cavity. The Hamiltonian of the

system reads ($\hbar = 1$)

$$H = \omega_c a^\dagger a + \sum_{l=1,2} \left(\frac{p_{xl}^2}{2m_l} + \frac{m_l \tilde{\omega}_l^2 x_l^2}{2} \right) - \lambda a^\dagger a x_1 + \eta (x_1 - x_2)^2 + \Omega (a^\dagger e^{-i\omega_L t} + a e^{i\omega_L t}), \quad (1)$$

where a and a^\dagger are, respectively, the annihilation and creation operators of the cavity mode with the resonance frequency ω_c . The coordinate and momentum operators x_l and p_{xl} are introduced to describe the l th ($l = 1, 2$) mechanical resonator with mass m_l and resonance frequency $\tilde{\omega}_l$. The optomechanical coupling between the cavity field and the first mechanical mode is described by the λ term in Eq. (1), where $\lambda = \omega_c/L$ denotes the optomechanical force of a single photon, with L being the rest length of the optical cavity. The η term depicts the mechanical interaction between the two mechanical resonators. The parameters ω_L and Ω are, respectively, the optical driving frequency and driving amplitude, which is determined by the driving power via the relation $\Omega = \sqrt{2P_L \kappa / \omega_L}$, where P_L is the power of the driving laser and κ is the decay rate of the cavity field.

For convenience, below we introduce the normalized resonance frequencies $\omega_{l=1,2} = \sqrt{\tilde{\omega}_l^2 + 2\eta/m_l}$ and the dimensionless position and momentum operators $q_{l=1,2} = \sqrt{m_l \omega_l} x_l$ and $p_{l=1,2} = \sqrt{1/(m_l \omega_l)} p_{xl}$ ($[q_l, p_l] = i$) for the mechanical resonators. Then, in the rotating frame defined by the unitary transformation operator $\exp(-i\omega_L t a^\dagger a)$, the Hamiltonian of the system becomes

$$H_I = \Delta_c a^\dagger a + \sum_{l=1,2} \frac{\omega_l}{2} (q_l^2 + p_l^2) - \lambda_0 a^\dagger a q_1 - 2\eta_0 q_1 q_2 + \Omega (a^\dagger + a), \quad (2)$$

where $\Delta_c = \omega_c - \omega_L$ is the driving detuning of the cavity field, and $\lambda_0 = \lambda \sqrt{1/(m_1 \omega_1)}$ and $\eta_0 = \eta \sqrt{1/(m_1 m_2 \omega_1 \omega_2)}$ denote the strength of the optomechanical coupling and the mechanical coupling in the dimensionless representation, respectively. The Hamiltonian (2) is the starting point of our consideration. Below, we will study the cooling performance by seeking the steady-state solution of the system.

III. THE LANGEVIN EQUATIONS

Quantum systems are inevitably coupled to their environments. To treat the damping and noise in our model, we consider the case where the optical mode is linearly coupled to a vacuum bath and the two mechanical modes experience the Brownian motion. In this case, the evolution of the system can be described by the Langevin equations,

$$\dot{a} = -[\kappa + i(\Delta_c - \lambda_0 q_1)]a - i\Omega + \sqrt{2\kappa} a_{\text{in}}, \quad (3a)$$

$$\dot{q}_l = \omega_l p_l, \quad l = 1, 2, \quad (3b)$$

$$\dot{p}_1 = -\omega_1 q_1 - \gamma_1 p_1 + \lambda_0 a^\dagger a + 2\eta_0 q_2 + \xi_1, \quad (3c)$$

$$\dot{p}_2 = -\omega_2 q_2 - \gamma_2 p_2 + 2\eta_0 q_1 + \xi_2, \quad (3d)$$

where κ and $\gamma_{l=1,2}$ are the decay rates of the cavity mode and the l th mechanical mode, respectively. The operators a_{in} (a_{in}^\dagger) and $\xi_{l=1,2}$ are the noise operator of the cavity field and the

Brownian force which acts on the l th mechanical resonator, respectively. These operators have zero mean values and the following correlation functions:

$$\langle a_{\text{in}}(t)a_{\text{in}}^\dagger(t') \rangle = \delta(t-t'), \quad \langle a_{\text{in}}^\dagger(t)a_{\text{in}}(t') \rangle = 0, \quad (4a)$$

$$\langle \xi_l(t)\xi_l(t') \rangle = \frac{\gamma_l}{\omega_l} \int \frac{d\omega}{2\pi} e^{-i\omega(t-t')} \omega \left[\coth\left(\frac{\omega}{2k_B T_l}\right) + 1 \right], \quad (4b)$$

where k_B is the Boltzmann constant, and $T_{l=1,2}$ is the bath temperature of the l th mechanical resonator.

To cool the mechanical resonators, we consider the strong-driving regime of the cavity such that the average photon number in the cavity is sufficient large and then the linearization procedure can be used to simplify the physical model. To this end, we express the operators in Eq. (3) as the sum of their steady-state mean values and quantum fluctuations, namely, $o = \langle o \rangle_{\text{ss}} + \delta o$ for operators a , a^\dagger , $q_{l=1,2}$, and $p_{l=1,2}$. By separating the classical motion and the quantum fluctuation, the linearized equations of motion for the quantum fluctuations can be written as

$$\delta \dot{a} = -(\kappa + i\Delta)\delta a + iG\delta q_1 + \sqrt{2\kappa}a_{\text{in}}, \quad (5a)$$

$$\delta \dot{q}_l = \omega_l \delta p_l, \quad l = 1, 2, \quad (5b)$$

$$\delta \dot{p}_1 = -\omega_1 \delta q_1 - \gamma_1 \delta p_1 + 2\eta_0 \delta q_2 + G^* \delta a + G \delta a^\dagger + \xi_1, \quad (5c)$$

$$\delta \dot{p}_2 = -\omega_2 \delta q_2 - \gamma_2 \delta p_2 + 2\eta_0 \delta q_1 + \xi_2, \quad (5d)$$

where $\Delta = \Delta_c - \lambda_0 \langle q_1 \rangle_{\text{ss}}$ is the driving detuning normalized by the linearization and $G = \lambda_0 \langle a \rangle_{\text{ss}}$ denotes the strength of the linearized optomechanical coupling. Here, the steady-state solution of the quantum Langevin equations in Eq. (3) can be obtained as

$$\langle a \rangle_{\text{ss}} = \frac{-i\Omega}{\kappa + i\Delta}, \quad (6a)$$

$$\langle q_1 \rangle_{\text{ss}} = \frac{\lambda_0 \omega_2 \langle a^\dagger \rangle_{\text{ss}} \langle a \rangle_{\text{ss}}}{\omega_1 \omega_2 - 4\eta_0^2}, \quad (6b)$$

$$\langle q_2 \rangle_{\text{ss}} = \frac{2\lambda_0 \eta_0 \langle a^\dagger \rangle_{\text{ss}} \langle a \rangle_{\text{ss}}}{\omega_1 \omega_2 - 4\eta_0^2}, \quad (6c)$$

$$\langle p_1 \rangle_{\text{ss}} = \langle p_2 \rangle_{\text{ss}} = 0. \quad (6d)$$

The cooling problem can be solved by calculating the steady-state solution of Eq. (5). This can be realized by solving the variables in the frequency domain with the Fourier transformation method. Under the definition for operator r ($r = \delta a$, δq_l , δp_l , a_{in} , ξ) and its conjugate r^\dagger ,

$$r(t) = \frac{1}{\sqrt{2\pi}} \int_{-\infty}^{\infty} e^{i\omega t} \tilde{r}(\omega) d\omega, \quad (7a)$$

$$r^\dagger(t) = \frac{1}{\sqrt{2\pi}} \int_{-\infty}^{\infty} e^{-i\omega t} \tilde{r}^\dagger(\omega) d\omega, \quad (7b)$$

the equations of motion (5) can be expressed in the frequency domain as

$$i\omega \delta \tilde{a}(\omega) = -(\kappa + i\Delta)\delta \tilde{a}(\omega) + iG\delta \tilde{q}_1(\omega) + \sqrt{2\kappa}\tilde{a}_{\text{in}}(\omega), \quad (8a)$$

$$i\omega \delta \tilde{q}_l(\omega) = \omega_l \delta \tilde{p}_l(\omega), \quad l = 1, 2, \quad (8b)$$

$$i\omega \delta \tilde{p}_1(\omega) = -\omega_1 \delta \tilde{q}_1(\omega) - \gamma_1 \delta \tilde{p}_1(\omega) + G^* \delta \tilde{a}(\omega) + G \delta \tilde{a}^\dagger(\omega) + 2\eta_0 \delta \tilde{q}_2(\omega) + \tilde{\xi}_1(\omega), \quad (8c)$$

$$i\omega \delta \tilde{p}_2(\omega) = -\omega_2 \delta \tilde{q}_2(\omega) - \gamma_2 \delta \tilde{p}_2(\omega) + 2\eta_0 \delta \tilde{q}_1(\omega) + \tilde{\xi}_2(\omega), \quad (8d)$$

which can be further solved as

$$\begin{aligned} \delta \tilde{a}(\omega) = & \{iGC_1(\omega)\tilde{a}_{\text{in}}^\dagger(\omega) + [iGC_1^*(-\omega) + \sqrt{2\kappa}B(\omega)] \\ & \times \tilde{a}_{\text{in}}(\omega) + iGW_1(\omega)\tilde{\xi}_1(\omega) + iGW_2(\omega)\tilde{\xi}_2(\omega)\} \\ & \times [\kappa + i(\Delta + \omega)]^{-1} B^{-1}(\omega), \end{aligned} \quad (9a)$$

$$\begin{aligned} \delta \tilde{q}_1(\omega) = & [C_1(\omega)\tilde{a}_{\text{in}}^\dagger(\omega) + C_1^*(-\omega)\tilde{a}_{\text{in}}(\omega) + W_1(\omega)\tilde{\xi}_1(\omega) \\ & + W_2(\omega)\tilde{\xi}_2(\omega)]B^{-1}(\omega), \end{aligned} \quad (9b)$$

$$\begin{aligned} \delta \tilde{q}_2(\omega) = & [C_2(\omega)\tilde{a}_{\text{in}}^\dagger(\omega) + C_2^*(-\omega)\tilde{a}_{\text{in}}(\omega) + W_2(\omega)\tilde{\xi}_1(\omega) \\ & + W_3(\omega)\tilde{\xi}_2(\omega)]B^{-1}(\omega), \end{aligned} \quad (9c)$$

where we introduced the variables

$$\begin{aligned} B(\omega) = & (i\gamma_1\omega - \omega^2 + \omega_1^2)(-i\gamma_2\omega + \omega^2 - \omega_2^2)[(\kappa + i\omega)^2 \\ & + \Delta^2] + 2\omega_1(i\gamma_2\omega - \omega^2 + \omega_2^2)|G|^2\Delta \\ & + 4\omega_1\omega_2\eta_0^2[(\kappa + i\omega)^2 + \Delta^2], \end{aligned} \quad (10a)$$

$$C_1(\omega) = \sqrt{2\kappa}G\omega_1[\gamma_2\omega + i(\omega^2 - \omega_2^2)](-i\kappa + \omega + \Delta), \quad (10b)$$

$$C_2(\omega) = -2\sqrt{2\kappa}\eta_0G\omega_1\omega_2[\kappa + i(\omega + \Delta)], \quad (10c)$$

$$W_1(\omega) = \omega_1(-i\gamma_2\omega + \omega^2 - \omega_2^2)[(\kappa + i\omega)^2 + \Delta^2], \quad (10d)$$

$$W_2(\omega) = -2\eta_0\omega_1\omega_2[(\kappa + i\omega)^2 + \Delta^2], \quad (10e)$$

$$\begin{aligned} W_3(\omega) = & 2\omega_1\omega_2|G|^2\Delta + \omega_2(-i\gamma_1\omega + \omega^2 - \omega_1^2) \\ & \times [(\kappa + i\omega)^2 + \Delta^2]. \end{aligned} \quad (10f)$$

In principle, the expressions of these quantum fluctuations δa , $\delta q_{l=1,2}$, and $\delta p_{l=1,2}$ in the time domain can be calculated by performing the inverse Fourier transformation. For our cooling task, we will focus on the steady-state mean values of the phonon numbers in the mechanical resonators.

In the above consideration, we do the linearization around the steady state of the system. Therefore, we need to analyze the stability of the system. By applying the Routh-Hurwitz criterion [65], it is found that the stability condition, under which the system reaches a steady state, is given by

$$\Delta_6 > 0, \quad (11)$$

where the expression of Δ_6 is defined in Eq. (A6). In the following consideration, all the used parameters satisfy this stability condition.

IV. COOLING OF TWO MECHANICAL RESONATORS

In this section, we study the cooling efficiency of the mechanical resonators by calculating the final mean phonon numbers and deriving the cooling limits.

A. The final mean phonon numbers

For the purpose of quantum cooling, we prefer to calculate the fluctuation spectra of the position and momentum operators for the two mechanical resonators, and then the final mean phonon numbers in the mechanical resonators can be obtained by integrating the corresponding fluctuation spectra. Mathematically, the final mean phonon numbers in the two mechanical resonators can be calculated by the relation [45]

$$n_l^f = \frac{1}{2} [\langle \delta q_l^2 \rangle + \langle \delta p_l^2 \rangle - 1], \quad (12)$$

where the variances δq_l^2 and δp_l^2 of the position and momentum operators can be obtained by solving Eq. (8) in the frequency domain and integrating the corresponding fluctuation spectra,

$$\langle \delta q_l^2 \rangle = \frac{1}{2\pi} \int_{-\infty}^{\infty} S_{q_l}(\omega) d\omega, \quad l = 1, 2, \quad (13a)$$

$$\begin{aligned} \langle \delta p_l^2 \rangle &= \frac{1}{2\pi} \int_{-\infty}^{\infty} S_{p_l}(\omega) d\omega \\ &= \frac{1}{2\pi\omega_l^2} \int_{-\infty}^{\infty} \omega^2 S_{q_l}(\omega) d\omega, \quad l = 1, 2. \end{aligned} \quad (13b)$$

Here the fluctuation spectra of the position and momentum of the two mechanical oscillators are defined by

$$S_o(\omega) = \int_{-\infty}^{\infty} e^{-i\omega\tau} \langle \delta o(t+\tau) \delta o(t) \rangle_{ss} d\tau, \quad (14)$$

for $o = q_{l=1,2}$ and $p_{l=1,2}$. Here the average $\langle \cdot \rangle_{ss}$ are taken over the steady state of the system. The fluctuation spectrum can also be expressed in the frequency domain as

$$\langle \delta \tilde{o}(\omega) \delta \tilde{o}(\omega') \rangle_{ss} = S_o(\omega) \delta(\omega + \omega') \quad (o = q_l, p_l). \quad (15)$$

Based on the results given in Eqs. (9) and (15), and the correlation function (4) in the frequency domain, the position and momentum fluctuation spectra of the mechanical resonators can be obtained as

$$\begin{aligned} S_{q_1}(\omega) &= \frac{1}{|B(\omega)|^2} \left\{ |C_1(\omega)|^2 \right. \\ &\quad + |W_1(\omega)|^2 \frac{\gamma_1 \omega}{\omega_1} \left[1 + \coth \left(\frac{\omega}{2k_B T_1} \right) \right] \\ &\quad \left. + |W_2(\omega)|^2 \frac{\gamma_2 \omega}{\omega_2} \left[1 + \coth \left(\frac{\omega}{2k_B T_2} \right) \right] \right\}, \end{aligned} \quad (16a)$$

$$\begin{aligned} S_{q_2}(\omega) &= \frac{1}{|B(\omega)|^2} \left\{ |C_2(\omega)|^2 \right. \\ &\quad + |W_2(\omega)|^2 \frac{\gamma_1 \omega}{\omega_1} \left[1 + \coth \left(\frac{\omega}{2k_B T_1} \right) \right] \\ &\quad \left. + |W_3(\omega)|^2 \frac{\gamma_2 \omega}{\omega_2} \left[1 + \coth \left(\frac{\omega}{2k_B T_2} \right) \right] \right\}, \end{aligned} \quad (16b)$$

$$S_{p_l}(\omega) = \left(\frac{\omega}{\omega_l} \right)^2 S_{q_l}(\omega), \quad l = 1, 2. \quad (16c)$$

In terms of Eqs. (12), (13), and (16), the exact analytical results of the final mean phonon numbers in the two mechanical resonators can be obtained (see Appendix A for details).

B. Ground-state cooling

Based on the above results, we now study the cooling of the two coupled mechanical resonators by the optomechanical coupling. Physically, the system becomes, by linearization, a chain of three modes with the bilinear-type coupling between the neighboring modes. As a result, the excitation energy can be exchanged between the two neighboring modes by the rotating-wave term (namely, the beam-splitter-type coupling) in the near-resonance and weak-coupling regimes. In this system, the two mechanical resonators are connected to two heat baths and the cavity field is connected to a vacuum bath. Hence the final mean phonon numbers in the two mechanical resonators would be finite numbers, which should be smaller than the thermal phonon occupations in the heat baths because the thermal excitations can be finally extracted to the vacuum bath. In this sense, the mechanical resonators can be cooled by the optomechanical coupling. Below, we will show how the final mean phonon numbers in the two mechanical resonators depend on the parameters of the system.

In Fig. 2, we plot the final mean phonon numbers n_1^f and n_2^f as a function of the driving detuning Δ/ω_1 and the cavity-field decay rate κ/ω_1 . Here we choose the mechanical frequency ω_1 as the frequency scale so that we can clearly see the relationship between the optimal driving detuning and the phonon sidebands, and the influence of the sideband-resolution condition on the cooling performance. When $\kappa/\omega_1 \ll 1$, the phonon sidebands can be resolved from the cavity-emission spectrum, and this regime is called the resolved-sideband limit. We can see from Fig. 2 that the two resonators can be cooled efficiently ($n_1^f, n_2^f \ll 1$) in the resolved-sideband limit and under the driving $\Delta/\omega_1 \sim 1$, which means that the ground-state cooling is achievable in this system. For the used parameters, the minimum phonon numbers for the two resonators are $n_1^f \approx 0.15$ and $n_2^f \approx 0.35$. For a given value of the ratio κ/ω_1 , the optimal driving detuning is given by $\Delta \approx \omega_1$. This is because the energy extraction efficiency between the cavity mode and the first mechanical mode should be maximum at $\Delta = \omega_1$, and the small deviation of the exact value of ω_1 in realistic simulations is caused by the counter-rotating-wave term in the linearized interaction between the cavity mode and the first mechanical mode. Physically, the generation of an anti-Stokes photon will cool the mechanical oscillator by taking away a phonon from the mechanical resonator. For the optimal cooling detuning $\Delta \approx \omega_1$, the frequency ω_1 of the phonon exactly matches the driving detuning Δ and hence $\Delta/\omega_1 = 1$ corresponds to the optimal cooling. At the optimal driving $\Delta = \omega_1$, the final mean phonon numbers become worse with the increase of the ratio κ/ω_1 . In order to clearly illustrate the dependence of the mean phonon numbers on the parameters, we show a rough boundary of ground-state cooling (n_1^f and $n_2^f = 1$), as shown by the black solid curves in Figs. 2(a)

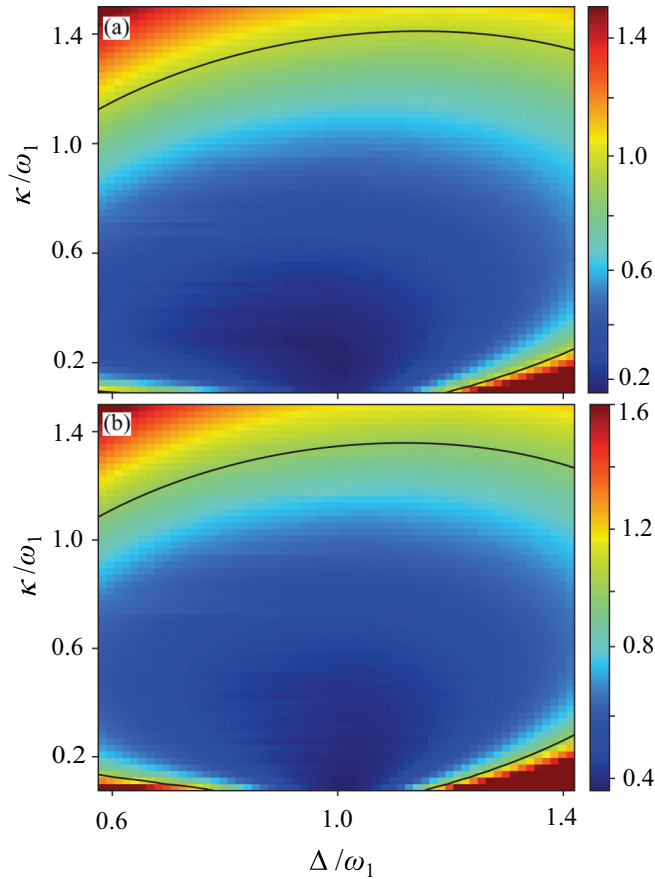


FIG. 2. The final mean phonon numbers (a) n_1^f and (b) n_2^f in the two mechanical resonators vs the effective driving detuning Δ/ω_1 and the decay rate κ/ω_1 . The used parameters are given by $\omega_1/2\pi = \omega_2/2\pi = 10$ MHz, $\gamma_1/\omega_1 = \gamma_2/\omega_1 = 10^{-5}$, $\omega_c/\omega_1 = 2.817 \times 10^7$, $\eta_0/\omega_1 = 0.04$, $m_1 = m_2 = 250$ ng, $\bar{n}_1 = \bar{n}_2 = 1000$, $L = 0.5$ mm, $P_L = 50$ mW, and $\lambda = 1064$ nm. The black solid curves correspond to $n_1^f = n_2^f = 1$.

and 2(b). These results are consistent with the sideband cooling results in a typical optomechanical system [41,42,45,46].

Since the cavity provides the direct channel to extract the thermal excitations in the first mechanical resonator, the optimal driving (corresponding to a resonant beam-splitter-type interaction) is important to the cooling efficiency. At the same time, the coupling between the two mechanical resonators provides the channel to extract the thermal excitations from the second mechanical resonator, as a cascade-cooling process. Consequently, the cooling efficiency of the second mechanical resonator should depend on the rotating-wave coupling between the two mechanical resonators, which is determined by the resonance frequencies of the two resonators and the coupling strength between them. To see this effect, in Fig. 3 we plot the final mean phonon numbers n_1^f and n_2^f as a function of the mechanical coupling strength η_0 between the two resonators when the cavity decay rate takes different values. Based on the fact that the second mechanical resonator will not be cooled at $\eta_0 = 0$, we confirm that the coupling between the two mechanical resonators provides the cooling channel for the second resonator. With the increase of η_0 ,

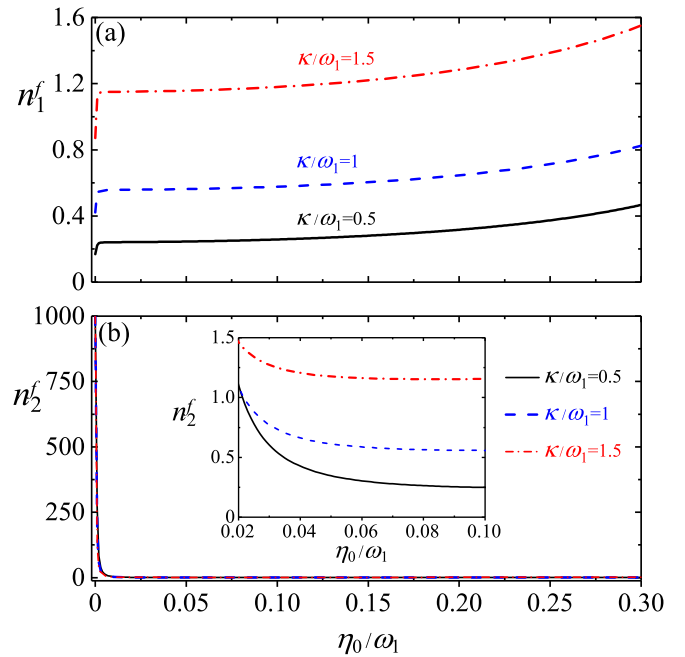


FIG. 3. The final mean phonon numbers (a) n_1^f and (b) n_2^f as a function of η_0/ω_1 when the cavity-field decay rate takes different values $\kappa/\omega_1 = 0.5, 1$, and 1.5 . The inset in (b) is a zoomed-in plot of n_2^f as a function of η_0/ω_1 , which clearly shows the dependence of n_2^f on the cavity-field decay rate. Here we consider the optimal driving case $\Delta = \omega_1$, and other parameters are the same as those used in Fig. 2.

the phonon number n_1^f increases, while the phonon number n_2^f decreases. This is because the first resonator provides the cool channel of the second resonator by extracting its thermal excitations, while the second resonator will encumber the cooling efficiency of the first resonator. Additionally, the final mean phonon numbers are larger for larger values of the decay rate κ/ω_1 , which is consistent with the analyses concerning the dependence of the cooling efficiency on the sideband-resolution condition.

This cascade-cooling process can also be seen by considering the case where the two mechanical resonators have different resonance frequencies. In Fig. 4, we display the dependence of the final mean phonon numbers n_1^f and n_2^f on the frequency ω_2 of the second resonator. Here we choose $\Delta = \omega_1$ such that the cooling efficiency of the first resonator is optimal. The result shows that both of the resonators have good cooling efficiency when the two resonators are resonant and near resonant (ω_2 around ω_1). With the increase of the detuning between the two resonance frequencies, the cooling efficiency becomes worse. The reason for this phenomenon is that the efficiency of energy extraction from the second resonator decreases with the increase of the detuning $|\omega_1 - \omega_2|$, and that the counter-rotating-wave interaction terms, which simultaneously create phonon excitations in the two resonators, become important when the frequency detuning becomes comparable to the mechanical frequencies. When $\omega_2/\omega_1 > 2$, the cooling of the second resonator is almost turned off because the interaction between the two resonators is approximately negligible under the condition $\eta_0/|\omega_1 - \omega_2| \ll 1$. In this case, the cooling of the

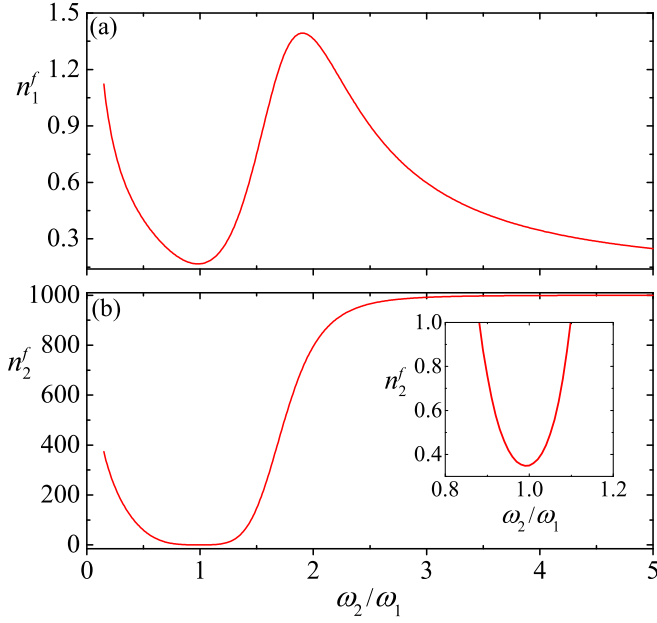


FIG. 4. The final mean phonon numbers (a) n_1^f and (b) n_2^f vs the ratio ω_2/ω_1 . The inset in (b) is a zoomed-in plot of n_2^f as a function of ω_2/ω_1 from 0.8 to 1.2. Here we choose $\Delta = \omega_1$ and $\kappa/\omega_1 = 0.2$. Other parameters are the same as those given in Fig. 2.

first resonator becomes better because the thermalization effect induced by the bath of the second resonator is turned off, and then the system is reduced to a typical optomechanical system with one cavity mode and one mechanical mode.

We note that the final mean phonon numbers n_1^f and n_2^f in the two resonators also depend on the mechanical decay rates γ_1 and γ_2 . In Fig. 5, we show the final phonon numbers as a function of the decay rates. Here we see that n_1^f and n_2^f increase with the increase of the mechanical decay rates. This is because the energy exchange rates between the mechanical resonators and their heat baths are faster for larger values of the decay rates, and then the thermal excitation in the heat bath will raise the phonon numbers in the mechanical resonators.

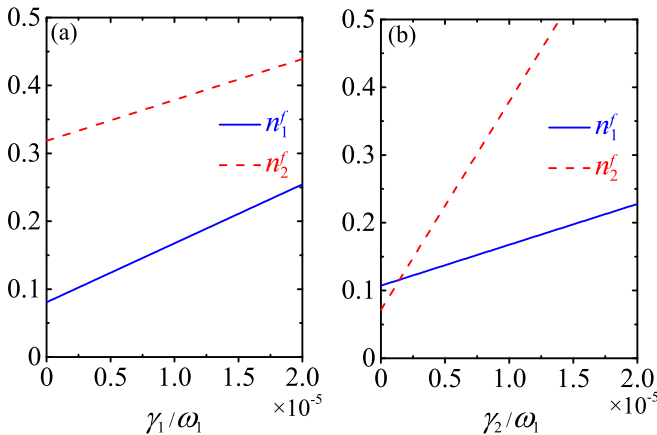


FIG. 5. The final mean phonon numbers n_1^f and n_2^f as a function of (a) γ_1 and (b) γ_2 . Here we take $\Delta = \omega_1$ and $\kappa/\omega_1 = 0.2$. Other parameters are the same as those given in Fig. 2.

In the plots in this section, we see that the first mechanical resonator is cooled better than the second resonator, i.e., $n_1^f < n_2^f$ under the same parameters. This phenomenon is a physical consequence of the cascade-cooling process in this system. The vacuum bath of the cavity plays the role of the pool to absorb the thermal excitations extracted from the two mechanical resonators. The cavity extracts the thermal excitations from the first resonator and transfers the excitations to its vacuum bath. The first resonator extracts the thermal excitations from the second resonator. Each mechanical resonator is connected to an independent heat bath, and the two heat baths have the same temperature. Hence, the relation $n_1^f < n_2^f$ can be understood from the point of view of the nonequilibrium physical process.

C. The cooling limits

Our exact results show that the ground-state cooling (with $n_{1,2}^f \ll 1$) is achievable for the two mechanical resonators under proper parameters. However, the cooling limits (i.e., the smallest achievable phonon numbers) of the resonators remain unclear. In this section, we derive the approximate cooling results in the bad-cavity regime such that analytical expressions of the cooling limits can be obtained. This is achieved by eliminating adiabatically the cavity field in the large-decay regime ($\kappa \gg \tilde{G}$) and then calculating the final phonon numbers in the two mechanical modes under the rotating-wave approximation ($\omega_{1,2} \gg \tilde{G}$). In this case, the system is reduced to two coupled modes b_1 and b_2 , where mode b_1 is contacted with the optomechanical cooling channel (γ_{opt} and \bar{n}_{opt}) and one heat bath (γ_1 and \bar{n}_1), and mode b_2 is contacted with the heat bath (γ_2 and \bar{n}_2), as shown in Fig. 1(b). Without loss of generality, we assume that the resonance frequencies of two mechanical resonators are the same, namely, $\omega_1 = \omega_2 = \omega_m$. By a lengthy calculation (see Appendix B), the approximate expressions of the final mean phonon numbers can be obtained as

$$n_1^f \approx \frac{\gamma_1 \bar{n}_1}{\Gamma_1} + \frac{\gamma_{\text{opt}} \bar{n}_{\text{opt}} + \chi n_{1,\chi}}{\Gamma_1 - 4\chi}, \quad (17a)$$

$$n_2^f \approx \frac{\gamma_2 \bar{n}_2 + \chi n_{2,\chi}}{\chi + \gamma_2}, \quad (17b)$$

with

$$\bar{n}_{\text{opt}} = \frac{\kappa^2}{4(\omega_m + \Delta)^2}, \quad (18a)$$

$$n_{1,\chi} = \frac{\gamma_2 \bar{n}_2 (4\chi + \Gamma_1)}{(\Gamma_1 + \gamma_2)(\chi + \gamma_2)}, \quad (18b)$$

$$n_{2,\chi} = \frac{\gamma_1 \bar{n}_1 + \gamma_2 \bar{n}_2 + \gamma_{\text{opt}} \bar{n}_{\text{opt}}}{\Gamma_1 + \gamma_2}, \quad (18c)$$

where $\Gamma_1 = \gamma_1 + \gamma_{\text{opt}}$. We also introduce the effective decay rates $\gamma_{\text{opt}} = 4|\tilde{G}|^2/\kappa$ and $\chi = 4\eta_0^2/(\gamma_1 + \gamma_{\text{opt}})$ corresponding to the optomechanical channel and the mechanical coupling channel, respectively. The parameter relations in this case are

$$\omega_{1,2} \gg \kappa \gg \tilde{G} \gg \{\Gamma_1, \gamma_{\text{opt}}\} \gg \gamma_{1,2}. \quad (19)$$

In the optimal-detuning case $\Delta = \omega_m$, the corresponding cooling limits n_1^{lim} and n_2^{lim} can be obtained with $\bar{n}_{\text{opt}} = \kappa^2/(16\omega_m^2)$.

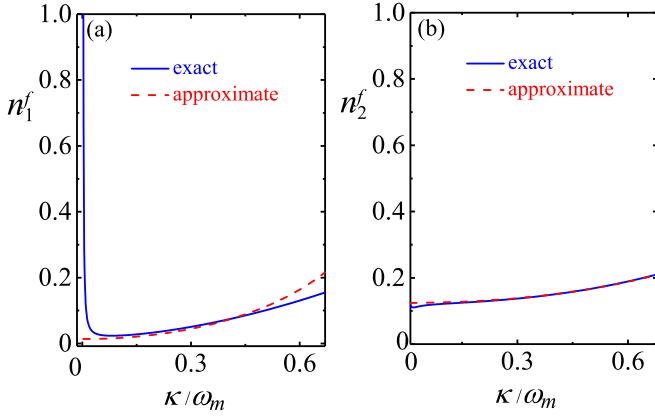


FIG. 6. The final mean phonon numbers (a) n_1^f and (b) n_2^f as a function of κ/ω_m . The exact results are given by Eq. (A5) (blue solid curve) and the approximate results obtained by the adiabatic elimination method are given by Eq. (17) (red dashed curve). In addition, we take $\Delta = \omega_m$, $\gamma_1/\omega_m = \gamma_2/\omega_m = 10^{-6}$, and $\eta_0/\omega_m = 0.02$. Other parameters are the same as those given in Fig. 2.

To evaluate the approximate cooling results, we compare the approximate results given in Eq. (17) with the exact results given in Eq. (A5). In Figs. 6 and 7, we plot the final mean phonon numbers n_1^f and n_2^f as a function of κ and η_0 when the optimal effective detuning $\Delta = \omega_m$. It shows that the approximate and exact mean phonon numbers coincide well with each other in $\kappa \approx 0.1\omega_m \sim 0.5\omega_m$ and $\eta_0 \approx 0 \sim 0.05\omega_m$. Figure 6(a) shows that the difference between the approximate result and the exact result increases when $\kappa < 0.1\omega_m$. This is because the adiabatic elimination procedure only works under the condition $\kappa \gg \tilde{G}$. In Fig. 7(a), we see that the two results do not match well for a large η_0 (for example, $\eta_0/\omega_m > 0.05$ in our simulations). This phenomenon can be explained based on the parameter requirement of the stability in the approximate analyses after the elimination of the cavity field. As shown in Eq. (B8), we can see that to ensure the stability of the equations of motion, the real part of the eigenvalues of the

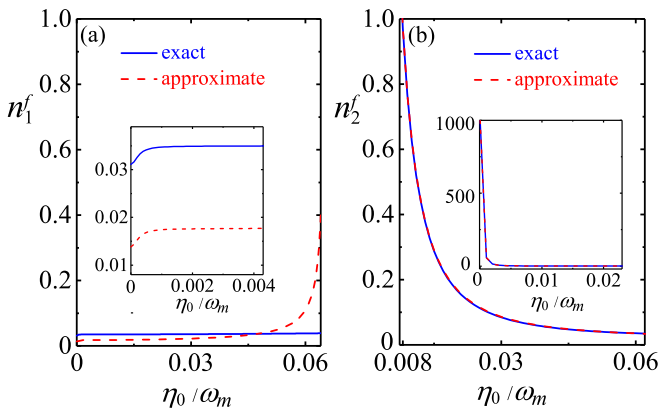


FIG. 7. The final mean phonon numbers (a) n_1^f and (b) n_2^f as a function of η_0/ω_m . The exact results (blue solid curve) and the approximate results (red dashed curve) are given by Eqs. (A5) and (17), respectively. The insets are zoom-in plots of the phonon numbers in a narrower range of η_0/ω_m . We take $\Delta = \omega_m$, $\kappa/\omega_m = 0.2$, and $P_L = 70$ mW. Other parameters are the same as those given in Fig. 6.

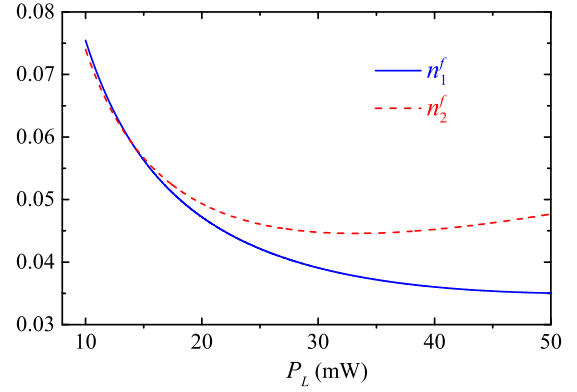


FIG. 8. The final average phonon numbers n_1^f and n_2^f in the two mechanical resonators vs the driving laser power P_L . The used parameters are given by $\Delta = \omega_m$, $\kappa/\omega_m = 0.2$, and $\gamma_{1,2}/\omega_m = 10^{-6}$. Other parameters are same as those used in Fig. 2.

coefficient matrix \mathbf{M} should be positive [65]. In the case of $\Omega_1 \approx \omega_2$ and $\gamma_1 = \gamma_2$, the parameter condition is reduced to $\gamma_{\text{opt}} > 4\chi$. Corresponding to Fig. 7(b), when $\eta_0/\omega_m > 0.05$, the stability condition $\gamma_{\text{opt}} > 4\chi$ of the equations of motion in the approximate analyses is violated.

The key physical mechanism in this cooling scheme is that the effective optical vacuum bath successively extracts the excitation energy from the two mechanical modes through the optomechanical cooling channel and the mechanical coupling channel. This physical picture can also be seen from the parameter relation $\gamma_{\text{opt}} > 4\chi \gg \gamma_{1,2}$, which indicates that the rate of the cooling channel should be much larger than the thermalization channel. The physical picture can also be seen by analyzing the following special cases. When we turn off the mechanical coupling channel, i.e., $\eta = 0$, then the first mechanical resonator will be cooled in the same manner as the typical optomechanical sideband cooling scheme [41,42], and the second resonator will be thermalized to a thermal equilibrium state at the same temperature as its bath.

In our above simulations, the final average phonon occupations in the mechanical resonators are smaller than 1. To better test interesting quantum effects in the resonators, the redundant single-phonon probability could be further suppressed by choosing mechanical resonators with smaller decay rates. In Fig. 8, we plot the final average phonon occupations n_1^f and n_2^f as a function of the laser power P_L when higher quality factors of the two resonators are taken (e.g., $Q_{l=1,2} = \omega_l/\gamma_l = 10^6$). Here we see that the phonon numbers in the two resonators can be effectively decreased from 1000 to 0.035 and 0.045, respectively. In these cases, the mechanical resonators are cooled to sufficiently low phonon number ($n_{1,2}^f \ll 1$) to test interesting quantum effects. This is because the mechanical resonators are prepared in their ground states with high fidelities.

V. COOLING OF A CHAIN OF COUPLED MECHANICAL RESONATORS

In this section, we extend the optomechanical cooling means to the cooling of a coupled-mechanical-resonator chain. Concretely, we consider an optomechanical cavity coupled to

an array of N mechanical resonators connected in series. The nearest-neighboring mechanical resonators are coupled to each other through “position-position” coupling. Without loss of generality, we assume that all the mechanical resonators are identical, having the same frequency, decay rate, and thermal occupation number. Meanwhile, the couplings between the mechanical resonators are much smaller than the mechanical frequency and hence the rotating-wave approximation is justified. Similarly, we consider the strong driving case of the cavity and then perform the linearization procedure to the system. In this case, the Hamiltonian of the system can be written in a frame rotating at the driving frequency as

$$H_I = \Delta a^\dagger a + \omega_m \sum_{j=1}^N b_j^\dagger b_j - (G a^\dagger b_1 + G^* b_1^\dagger a) - \sum_{j=1}^{N-1} \eta_0 (b_j^\dagger b_{j+1} + b_{j+1}^\dagger b_j) + \Omega (a^\dagger + a), \quad (20)$$

where a (a^\dagger) and $b_{j=1-N} = (q_j + ip_j)/\sqrt{2}$ [$b_j^\dagger = (q_j - ip_j)/\sqrt{2}$] are the annihilation (creation) operators of the cavity mode and the j th resonator. The parameter Δ is the driving detuning after the linearization of the optomechanical coupling, G is the strength of the linearized optomechanical coupling, and ω_m and η_0 are the frequency of these resonators and the coupling strength between the neighboring mechanical resonators, respectively. To include the dissipations, we assume that the cavity is coupled to a vacuum bath and the mechanical resonators are coupled to independent heat baths at the same temperatures. Then the evolution of the system can be governed by the quantum master equation

$$\begin{aligned} \dot{\rho} = & i[\rho, H_I] + \frac{\kappa}{2}(2a\rho a^\dagger - a^\dagger a\rho - \rho a^\dagger a) \\ & + \frac{\gamma_m}{2}(\bar{n}_m + 1) \sum_{j=1}^N (2b_j\rho b_j^\dagger - b_j^\dagger b_j\rho - \rho b_j^\dagger b_j) \\ & + \frac{\gamma_m \bar{n}_m}{2} \sum_{j=1}^N (2b_j^\dagger \rho b_j - b_j b_j^\dagger \rho - \rho b_j b_j^\dagger), \end{aligned} \quad (21)$$

where ρ is the density matrix of the coupled cavity-resonator system, \bar{n}_m is thermal phonon number of the heat baths of these mechanical resonators, and κ and γ_m are the decay rates of the cavity mode and the mechanical resonators, respectively.

To evaluate the cooling efficiency, we solve the steady-state solution of quantum master equation (21) and calculate the average occupation numbers in the cavity and these mechanical resonators. As examples, we consider the cases of three and four mechanical resonators (i.e., $N = 3, 4$) in our simulations. In Fig. 9, we plot the final mean phonon numbers in these mechanical resonators as a function of the effective driving detuning Δ for the cases of (a) $N = 3$ and (b) $N = 4$. We see that the ground-state cooling is achievable and the final phonon numbers successively increase from n_1^f to n_N^f at the optimal effective detuning $\Delta = \omega_m$. This means that the closer to the optomechanical cavity the resonator is, the smaller the final phonon number in this resonator is. The physical reason for this phenomenon is that the system is a cascade system and the vacuum bath of the optomechanical cavity provides the cooling

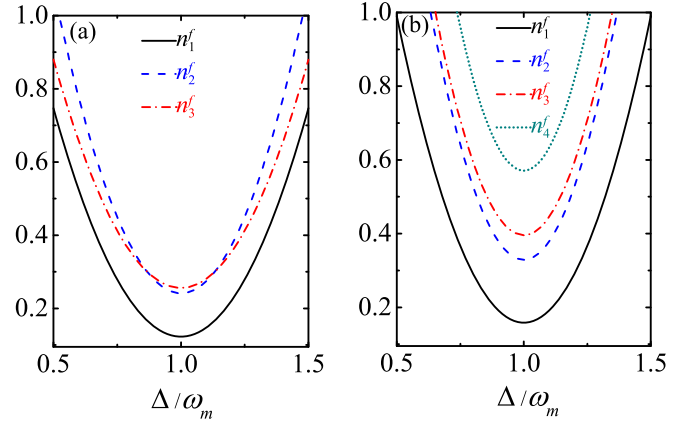


FIG. 9. The final mean phonon numbers in the mechanical resonators as a function of the effective driving detuning Δ when (a) $N = 3$ and (b) $N = 4$. Other parameters are given by $G/\omega_m = 0.2$, $\eta_0/\omega_m = 0.1$, $\kappa/\omega_m = 0.3$, $\gamma_m/\omega_m = 10^{-5}$, and $\bar{n} = 1000$.

reservoir to extract the thermal excitations in these mechanical resonators, which are thermally excited by their heat baths. After the linearization, the system is reduced to an array of coupled bosonic modes. Then the vacuum bath provides the cooling channel of the cavity, and the cavity provides the cooling channel of the first mechanical resonator. Successively, the former resonator provides the cooling channel for the next resonator. In this way, the thermal occupations can be extracted to the vacuum bath and then the system approaches to a nonequilibrium steady state. As a result, the cooling efficiency is higher for a mechanical oscillator which is closer to the cavity.

VI. DISCUSSIONS AND CONCLUSION

Finally, we present some discussions on the understanding of the cooling problem in the mechanical normal-mode representation. In our system, the first mechanical resonator is coupled to the cavity field through the radiation-pressure interaction, and the neighboring mechanical resonators are coupled to each other by the so-called position-position coupling. By diagonalizing the coupled mechanical resonators, the present physical model is reduced to a multimode optomechanical model which is composed of a single-mode cavity field coupled to all the mechanical normal modes [60]. In the presence of the mechanical coupling, the frequencies of these normal modes are different, and this hence provides a natural method to remove the dark-mode effect, which is a major obstacle of the cooling of many mechanical resonators coupled to a common cavity [60]. In principle, we can calculate the cooling problem in the representation of the mechanical normal modes. However, the physical mechanism could be explained clearly in the cascade-cooling picture because we consider the cooling of these mechanical resonators in the bare-mode representation.

It is worthwhile to present some discussions of the relationship between the coupled-mechanical-resonator system and the multiple modes in a single-mechanical-resonator system. In a realistic single-mechanical-resonator system, there are many normal modes with different resonance frequencies and these normal modes decouple from each other. Therefore, each of these normal modes can be cooled to its quantum ground

state by introducing the optomechanical cooling scheme. In a coupled-mechanical-resonator system, these coupled mechanical resonators can be diagonalized and then this system can be described by a similar Hamiltonian as that of the single-mechanical-resonator system. Basing on the fact that the frequencies of these diagonalized mechanical modes are governed by the coupling strength between these coupled mechanical resonators, we can design proper driving fields for realizing ground-state cooling of these diagonalized mechanical modes. Here, the dark-mode effect induced by the many mechanical resonators coupled to a common cavity field should be avoided by utilizing the frequency differences among these coupled mechanical resonators.

In conclusion, we have proposed a scheme to realize the ground-state cooling of coupled mechanical resonators in a three-mode optomechanical system where an optomechanical cavity is coupled to another mechanical resonator. By the linearization, the system is reduced to a cascade-type three-mode coupled system; then the thermal excitations in the mechanical resonators can be extracted to the vacuum bath of the cavity and the system can be cooled by the optomechanical coupling channel. We found that the coupled mechanical resonators can be simultaneously cooled to their ground states when the system works in the resolved-sideband regime and under a proper driving frequency. In the large-decay limit, we derived analytical expressions of the cooling limits by adiabatically eliminating the cavity field. We also extend the optomechanical method to the cooling of a chain of coupled mechanical resonators. The numerical results show that the ground-state cooling is achievable in this system.

ACKNOWLEDGMENTS

D.-G.L. thanks Wang-Jun Lu for valuable discussions. J.-Q.L. thanks Professors David Vitali, Yong Li, Xin-You Lü, and Yong-Chun Liu for valuable discussions, and thanks Da Xu for reading the manuscript and helpful suggestions. J.-Q.L. thanks Dr. Claudiu Genes for pointing out the integral formula used in Ref. [45]. This work is supported in part by the National Natural Science Foundation of China under Grants No. 11822501, No. 11774087, No. 11505055, No. 11574398, and No. 11654003, and the Hunan Provincial Natural Science Foundation of China under Grant No. 2017JJ1021.

APPENDIX A: CALCULATION OF THE FINAL MEAN PHONON NUMBERS

In this appendix, we present the detailed calculations of the final mean phonon numbers in the two mechanical resonators. As shown in Sec. IV A, the exact results of the final mean

phonon numbers in the two mechanical resonators can be obtained by calculating the integral in Eq. (13) for the position and momentum fluctuation spectra. Below, we consider the high-temperature limit case $k_B T_l \gg \hbar \omega_{1,2}$; then it is safe to perform the approximation

$$\gamma_l \frac{\omega}{\omega_l} \coth\left(\frac{\hbar \omega}{2k_B T_l}\right) \approx \gamma_l (2\bar{n}_l + 1), \quad l = 1, 2. \quad (\text{A1})$$

In this case, the integral kernels in Eq. (13) take the form $g_n(\omega)/[h_n(\omega)h_n(-\omega)]$. This kind of integral can be calculated exactly by the following formula [65]:

$$\int_{-\infty}^{\infty} \frac{g_n(\omega)}{h_n(\omega)h_n(-\omega)} d\omega = \frac{i\pi}{a_0} \frac{M_n}{\Delta_n}, \quad (\text{A2})$$

where the functions $g_n(\omega)$ and $h_n(\omega)$ in the integral kernels take the form

$$\begin{aligned} g_n(\omega) &= b_0 \omega^{2n-2} + b_1 \omega^{2n-4} \cdots + b_{n-1}, \\ h_n(\omega) &= a_0 \omega^n + a_1 \omega^{n-1} \cdots + a_n, \end{aligned} \quad (\text{A3})$$

with $b_{0,1,2,\dots}$ and $a_{0,1,2,\dots}$ being the coefficients. The variables Δ_n and M_n in Eq. (A2) are defined by

$$\begin{aligned} \Delta_n &= \begin{vmatrix} a_1 & a_3 & a_5 & \cdots & 0 \\ a_0 & a_2 & a_4 & & 0 \\ 0 & a_1 & a_3 & & 0 \\ \vdots & & & \ddots & \\ 0 & 0 & 0 & & a_n \end{vmatrix}, \\ M_n &= \begin{vmatrix} b_0 & b_1 & b_2 & \cdots & b_{n-1} \\ a_0 & a_2 & a_4 & & 0 \\ 0 & a_1 & a_3 & & 0 \\ \vdots & & & \ddots & \\ 0 & 0 & 0 & & a_n \end{vmatrix}, \end{aligned} \quad (\text{A4})$$

where $|\cdot|$ stands for the determinant. By using the above formula, the integrals in Eq. (13) can be calculated exactly and then the final mean phonon numbers in the two mechanical resonators can be obtained as ($n = 6$ for our three-mode system)

$$\begin{aligned} n_1^f &= \frac{1}{2} \left(\frac{iD_6^{(1)}}{2\Delta_6} + \frac{iM_6^{(1)}}{2\Delta_6} - 1 \right), \\ n_2^f &= \frac{1}{2} \left(\frac{iD_6^{(2)}}{2\Delta_6} + \frac{iM_6^{(2)}}{2\Delta_6} - 1 \right). \end{aligned} \quad (\text{A5})$$

Here, we introduce the variables

$$\begin{aligned} \Delta_6 &= a_5 \{ a_4 (-a_1 a_2 a_3 + a_3^2 + a_1^2 a_4) + [-a_2 a_3 + a_1 (a_2^2 - 2a_4)] a_5 + a_5^2 \} - [a_3^3 - a_1 a_3 (a_2 a_3 + 3a_5) \\ &\quad + a_1^2 (a_3 a_4 + 2a_2 a_5)] a_6 + a_1^3 a_6^2, \end{aligned} \quad (\text{A6})$$

$$\begin{aligned} D_6^{(s=1,2)} &= [-a_3 a_4 a_5 + a_3^2 a_6 + a_5 (a_2 a_5 - a_1 a_6)] b_1^{(s)} + (a_1 a_4 a_5 - a_5^2 - a_1 a_3 a_6) b_2^{(s)} + (-a_1 a_2 a_5 + a_3 a_5 + a_1^2 a_6) b_3^{(s)} \\ &\quad + [-a_3^2 - a_1^2 a_4 + a_1 (a_2 a_3 + a_5)] b_4^{(s)} + \frac{1}{a_6} [a_3^2 a_4 - a_2 a_3 a_5 + a_5^2 + a_1^2 (a_4^2 - a_2 a_6) + a_1 (-a_2 a_3 a_4 + a_2^2 a_5 \\ &\quad - 2a_4 a_5 + a_3 a_6)] b_5^{(s)}, \end{aligned} \quad (\text{A7})$$

and

$$\begin{aligned}
M_6^{(s=1,2)} = & \frac{1}{\omega_s^2} \left(-\{a_5[-a_2a_3a_4 + a_2^2a_5 + a_4(a_1a_4 - a_0a_5)]\} + [-a_1a_3a_4 + a_0a_3a_5 + a_2(a_3^2 - 2a_1a_5)]a_6 + a_1^2a_6^2 \right) b_1^{(s)} \\
& + [-a_3a_4a_5 + a_3^2a_6 + a_5(a_2a_5 - a_1a_6)]b_2^{(s)} + (a_1a_4a_5 - a_5^2 - a_1a_3a_6)b_3^{(s)} + (-a_1a_2a_5 + a_3a_5 + a_1^2a_6)b_4^{(s)} \\
& + [-a_3^2 - a_1^2a_4 + a_1(a_2a_3 + a_5)]b_5^{(s)}, \tag{A8}
\end{aligned}$$

where the coefficients in our three-mode system are defined by

$$\begin{aligned}
a_0 &= 1, \\
a_1 &= -i(2\kappa + \gamma_1 + \gamma_2), \\
a_2 &= -[\kappa^2 + \gamma_1\gamma_2 + \omega_1^2 + \omega_2^2 + \Delta^2 + 2\kappa(\gamma_1 + \gamma_2)], \\
a_3 &= i[(\kappa^2 + \Delta^2)(\gamma_1 + \gamma_2) + 2\kappa(\gamma_1\gamma_2 + \omega_1^2 + \omega_2^2) + \gamma_2\omega_1^2 + \gamma_1\omega_2^2], \\
a_4 &= (\kappa^2 + \Delta^2)(\gamma_1\gamma_2 + \omega_1^2 + \omega_2^2) + 2\kappa(\gamma_2\omega_1^2 + \gamma_1\omega_2^2) + \omega_1\omega_2(\omega_1\omega_2 - 4\eta_0^2) - 2\omega_1|G|^2\Delta, \\
a_5 &= -i\{\kappa^2(\gamma_2\omega_1^2 + \gamma_1\omega_2^2) + 2\kappa\omega_1\omega_2(\omega_1\omega_2 - 4\eta_0^2) + \Delta[\gamma_1\omega_2^2\Delta + \gamma_2\omega_1(-2|G|^2 + \omega_1\Delta)]\}, \\
a_6 &= \omega_1\omega_2\{\Delta[2\omega_2|G|^2 - \omega_1\omega_2\Delta + 4\eta_0^2\Delta] + \kappa^2(-\omega_1\omega_2 + 4\eta_0^2)\}, \tag{A9}
\end{aligned}$$

$$b_0^{(1)} = 0,$$

$$b_1^{(1)} = (1 + 2\bar{n}_1)\gamma_1\omega_1^2,$$

$$b_2^{(1)} = b_1^{(1)}[2\kappa^2 + \gamma_2^2 - 2(\omega_2^2 + \Delta^2)] + 2\omega_1^2\kappa|G|^2,$$

$$b_3^{(1)} = b_1^{(1)}[\kappa^4 + 2\kappa^2(\gamma_2^2 - 2\omega_2^2 + \Delta^2) + \omega_2^4 - 2\gamma_2^2\Delta^2 + \Delta^4 + 4\omega_2^2\Delta^2] + 4b_1^{(2)}\eta_0^2\omega_1^2 + 2\omega_1^2|G|^2\kappa[\kappa^2 + \gamma_2^2 - 2\omega_2^2 + \Delta^2],$$

$$b_4^{(1)} = b_1^{(1)}[2\omega_2^4(\kappa^2 - \Delta^2) + (\gamma_2^2 - 2\omega_2^2)(\kappa^2 + \Delta^2)^2] + 8b_1^{(2)}\eta_0^2\omega_1^2(\kappa^2 - \Delta^2) + 2\kappa\omega_1^2|G|^2[\omega_2^4 + (\gamma_2^2 - 2\omega_2^2)(\kappa^2 + \Delta^2)],$$

$$b_5^{(1)} = (b_1^{(1)}\omega_2^4 + 4b_1^{(2)}\eta_0^2\omega_1^2)(\kappa^2 + \Delta^2)^2 + 2\kappa\omega_1^2\omega_2^4(\kappa^2 + \Delta^2)|G|^2, \tag{A10}$$

and

$$b_0^{(2)} = 0,$$

$$b_1^{(2)} = (1 + 2\bar{n}_2)\gamma_2\omega_2^2,$$

$$b_2^{(2)} = b_1^{(2)}[2\kappa^2 + \gamma_1^2 - 2(\omega_1^2 + \Delta^2)],$$

$$b_3^{(2)} = b_1^{(2)}[\kappa^4 + 2\kappa^2(\gamma_1^2 - 2\omega_1^2 + \Delta^2) + \Delta^2(\Delta^2 - 2\gamma_1^2 + 4\omega_1^2) + \omega_1^4 - 4|G|^2\omega_1\Delta] + 4b_1^{(1)}\omega_2^2\eta_0^2,$$

$$\begin{aligned}
b_4^{(2)} = & b_1^{(2)}[4|G|^2\Delta\omega_1(2\kappa\gamma_1 + \kappa^2 + \omega_1^2 + \Delta^2) + (\gamma_1^2 - 2\omega_1^2)(\kappa^2 + \Delta^2)^2 + 2\omega_1^4(\kappa^2 - \Delta^2)] \\
& + 8b_1^{(1)}\omega_2^2\eta_0^2(\kappa^2 - \Delta^2) + 8|G|^2\kappa(\omega_1\omega_2\eta_0)^2,
\end{aligned}$$

$$\begin{aligned}
b_5^{(2)} = & b_1^{(2)}\omega_1^2\{\kappa^4\omega_1^2 + (-2|G|^2 + \omega_1\Delta)[-2|G|^2\Delta^2 + (\Delta^2 + 2\kappa^2)\omega_1\Delta]\} + 4b_1^{(1)}\omega_2^2\eta_0^2(\kappa^2 + \Delta^2)^2 \\
& + 8|G|^2\kappa(\omega_1\omega_2\eta_0)^2(\kappa^2 + \Delta^2). \tag{A11}
\end{aligned}$$

Note that the results given by Eq. (A5) are exact but complicated. In the large-decay regime, the cavity field can be adiabatically eliminated and we can then obtain analytical and concise expressions of the cooling limits.

APPENDIX B: DERIVATION OF EQS. (17)

In this appendix, we show a detailed derivation of the cooling limits, which are obtained by adiabatically eliminating the cavity field in the large-decay regime. For calculation convenience, we introduce the annihilation and creation operators of the mechanical modes as

$$b_{l=1,2} = (q_l + ip_l)/\sqrt{2}, \quad b_{l=1,2}^\dagger = (q_l - ip_l)/\sqrt{2}. \tag{B1}$$

The Hamiltonian (2) can then be expressed as

$$\begin{aligned}
H_I = & \Delta_c a^\dagger a + \sum_{l=1,2} \omega_l b_l^\dagger b_l - \eta_0(b_1^\dagger + b_1)(b_2^\dagger + b_2) \\
& - \frac{1}{\sqrt{2}} \lambda_0 a^\dagger a (b_1^\dagger + b_1) + \Omega(a^\dagger + a), \tag{B2}
\end{aligned}$$

where $\Delta_c = \omega_c - \omega_L$ denotes the detuning between the cavity frequency and the driving frequency. By performing the linearization, we write the operators of the system as a summation of their steady-state values and fluctuations: $a \rightarrow \langle a \rangle_{ss} + \delta a$, $b_1 \rightarrow \langle b_1 \rangle_{ss} + \delta b_1$ and $b_2 \rightarrow \langle b_2 \rangle_{ss} + \delta b_2$, where $\langle o \rangle_{ss}$ represents the steady-state value of the operator o , and

δa , δb_1 , and δb_2 are the corresponding fluctuations. The Langevin equations of these fluctuation operators become

$$\delta \dot{a} = (-\kappa/2 - i\Delta)\delta a + i\tilde{G}(\delta b_1^\dagger + \delta b_1) + \sqrt{\kappa}a_{\text{in}}, \quad (\text{B3a})$$

$$\delta \dot{b}_1 = (-\gamma_1/2 - i\omega_1)\delta b_1 + i\eta_0(\delta b_2^\dagger + \delta b_2) + (i\tilde{G}^*\delta a + i\tilde{G}\delta a^\dagger) + \sqrt{\gamma_1}b_{\text{in},1}, \quad (\text{B3b})$$

$$\delta \dot{b}_2 = (-\gamma_2/2 - i\omega_2)\delta b_2 + i\eta_0(\delta b_1^\dagger + \delta b_1) + \sqrt{\gamma_2}b_{\text{in},2}, \quad (\text{B3c})$$

where $\Delta = \Delta_c - \lambda_0(\langle b_1 \rangle_{\text{ss}}^* + \langle b_1 \rangle_{\text{ss}})/\sqrt{2}$ is the normalized detuning and $\tilde{G} = \lambda_0 \langle a \rangle_{\text{ss}}/\sqrt{2}$ is the strength of the linearized optomechanical coupling.

To obtain the cooling limits of the mechanical modes, we consider the parameter regime $\omega_{1,2} \gg \kappa \gg \tilde{G} \gg \gamma_{1,2}$. In this case, the cavity field can be eliminated adiabatically and then the solution of the operator $\delta a(t)$ at the timescale $t \gg 1/\kappa$ can be obtained as

$$\delta a(t) \approx \frac{i\tilde{G}}{\kappa/2 + i(\Delta + \omega_1)}\delta b_1^\dagger(t) + \frac{i\tilde{G}}{\kappa/2 + i(\Delta - \omega_1)}\delta b_1(t) + F_{a,\text{in}}(t), \quad (\text{B4})$$

where we introduce the noise operator

$$F_{a,\text{in}}(t) = \sqrt{\kappa}e^{-(\kappa/2+i\Delta)t} \int_0^t e^{(\kappa/2+i\Delta)s} a_{\text{in}}(s) ds. \quad (\text{B5})$$

Substitution of Eq. (B4) into Eqs. (B3b) and (B3c) leads to the equations of motion

$$\delta \dot{b}_1(t) = -(\Gamma_1/2 + i\Omega_1)\delta b_1(t) + i\eta_0\delta b_2(t) + i\tilde{G}^*F_{a,\text{in}}(t) + i\tilde{G}F_{a,\text{in}}^\dagger(t) + \sqrt{\gamma_1}b_{\text{in},1}(t), \quad (\text{B6a})$$

$$\delta \dot{b}_2(t) = i\eta_0\delta b_1(t) - (\gamma_2/2 + i\omega_2)\delta b_2(t) + \sqrt{\gamma_2}b_{\text{in},2}(t), \quad (\text{B6b})$$

where $\Gamma_1 = \gamma_1 + \gamma_{\text{opt}}$ and $\Omega_1 = \omega_1 - \omega_{\text{opt}}$ with $\gamma_{\text{opt}} = 4|\tilde{G}|^2/\kappa$ and $\omega_{\text{opt}} = |\tilde{G}|^2/(2\omega_1)$, which denote the decay rate and frequency shift induced by the cavity coupling channel, respectively.

The final mean phonon numbers (namely, the steady-state expected values of the phonon number operators) can be obtained by solving Eq. (B6). To be concise, we reexpress Eq. (B6) as

$$\dot{\mathbf{v}}(t) = -\mathbf{M}\mathbf{v}(t) + \mathbf{N}(t), \quad (\text{B7})$$

where $\mathbf{v}(t) = [\delta b_1(t), \delta b_2(t)]^T$, and \mathbf{M} and $\mathbf{N}(t)$ are defined by

$$\mathbf{M} = \begin{pmatrix} \Gamma_1/2 + i\Omega_1 & -i\eta_0 \\ -i\eta_0 & \gamma_2/2 + i\omega_2 \end{pmatrix}, \quad \mathbf{N}(t) = \begin{pmatrix} i\tilde{G}^*F_{a,\text{in}}(t) + i\tilde{G}F_{a,\text{in}}^\dagger(t) + \sqrt{\gamma_1}b_{\text{in},1}(t) \\ \sqrt{\gamma_2}b_{\text{in},2}(t) \end{pmatrix}. \quad (\text{B8})$$

The formal solution of Eq. (B7) can be written as

$$\mathbf{v}(t) = e^{-\mathbf{M}t}\mathbf{v}(0) + e^{-\mathbf{M}t} \int_{t_0}^t e^{\mathbf{M}s}\mathbf{N}(s) ds. \quad (\text{B9})$$

The final mean phonon numbers can be obtained by calculating the elements of the variance matrix. By a lengthy calculation, we obtain the approximate analytical expressions for the final mean phonon numbers as

$$\begin{aligned} n_1^f &= \frac{1}{4|u|^2} \left[\gamma_1 \bar{n}_1 \left(\frac{|u - 2(\Gamma_1 - \gamma_2) - 4i(\Omega_1 - \omega_2)|^2}{\lambda_1 + \lambda_1^*} + \frac{|u + 2(\Gamma_1 - \gamma_2) + 4i(\Omega_1 - \omega_2)|^2}{\lambda_2 + \lambda_2^*} \right) \right. \\ &\quad \left. + 2\text{Re} \left\{ \frac{[u - 2(\Gamma_1 - \gamma_2) - 4i(\Omega_1 - \omega_2)][u^* + 2(\Gamma_1 - \gamma_2) - 4i(\Omega_1 - \omega_2)]}{\lambda_1 + \lambda_2^*} \right\} \right] \\ &\quad + |\tilde{G}|^2 \left\{ \frac{(\kappa + \lambda_1^* + \lambda_1)|u - 2(\Gamma_1 - \gamma_2) - 4i(\Omega_1 - \omega_2)|^2}{(\lambda_1 + \lambda_1^*)|\frac{\kappa}{2} + \lambda_1 + i\Delta|^2} + \frac{(\kappa + \lambda_2^* + \lambda_2)|u + 2(\Gamma_1 - \gamma_2) + 4i(\Omega_1 - \omega_2)|^2}{(\lambda_2 + \lambda_2^*)|\frac{\kappa}{2} + \lambda_2 + i\Delta|^2} \right. \\ &\quad \left. + 2\text{Re} \left[\frac{(\kappa + \lambda_1 + \lambda_2^*)[u^* + 2(\Gamma_1 - \gamma_2) - 4i(\Omega_1 - \omega_2)][u - 2(\Gamma_1 - \gamma_2) - 4i(\Omega_1 - \omega_2)]}{(\lambda_1 + \lambda_2^*)(\frac{\kappa}{2} + \lambda_1 + i\Delta)(\frac{\kappa}{2} + \lambda_2^* - i\Delta)} \right] \right\} \\ &\quad + 64\eta_0^2 \gamma_2 \bar{n}_2 \frac{(\lambda_1 + \lambda_1^* + \lambda_2 + \lambda_2^*)[(\lambda_1^* + \lambda_2)(\lambda_1 + \lambda_2^*) + (\lambda_1 + \lambda_1^*)(\lambda_2 + \lambda_2^*)]}{(\lambda_1^* + \lambda_1)(\lambda_2^* + \lambda_2)(\lambda_1^* + \lambda_2)(\lambda_1 + \lambda_2^*)}, \end{aligned} \quad (\text{B10})$$

$$\begin{aligned} n_2^f &= \frac{1}{4|u|^2} \left[64\eta_0^2 \left(\gamma_1 \bar{n}_1 \frac{(\lambda_1 - \lambda_2)(\lambda_1^* - \lambda_2^*)(\lambda_1 + \lambda_1^* + \lambda_2 + \lambda_2^*)}{(\lambda_1^* + \lambda_1)(\lambda_2^* + \lambda_2)(\lambda_1^* + \lambda_2)(\lambda_1 + \lambda_2^*)} + |\tilde{G}|^2 \left\{ \frac{\kappa + \lambda_1 + \lambda_1^*}{(\lambda_1 + \lambda_1^*)|\frac{\kappa}{2} + \lambda_1 + i\Delta|^2} \right. \right. \right. \\ &\quad \left. \left. + \frac{\kappa + \lambda_2 + \lambda_2^*}{(\lambda_2 + \lambda_2^*)|\frac{\kappa}{2} + \lambda_2 + i\Delta|^2} - 2\text{Re} \left[\frac{\kappa + \lambda_1 + \lambda_2^*}{(\lambda_1 + \lambda_2^*)(\frac{\kappa}{2} + \lambda_1 + i\Delta)(\frac{\kappa}{2} + \lambda_2^* - i\Delta)} \right] \right\} \right) \end{aligned}$$

$$\begin{aligned}
& + \gamma_2 \bar{n}_2 \left\{ \frac{|u + 2(\Gamma_1 - \gamma_2) + 4i(\Omega_1 - \omega_2)|^2}{\lambda_1 + \lambda_1^*} + \frac{|u - 2(\Gamma_1 - \gamma_2) - 4i(\Omega_1 - \omega_2)|^2}{\lambda_2 + \lambda_2^*} \right. \\
& \left. + 2\text{Re} \left[\frac{[u^* - 2(\Gamma_1 - \gamma_2) + 4i(\Omega_1 - \omega_2)][u + 2(\Gamma_1 - \gamma_2) + 4i(\Omega_1 - \omega_2)]}{\lambda_1 + \lambda_2^*} \right] \right\}, \quad (\text{B11})
\end{aligned}$$

where λ_1 and λ_2 (λ_1^* and λ_2^* are complex conjugate) are the eigenvalues of the coefficient matrix \mathbf{M} ,

$$\lambda_{1,2} = \frac{1}{4}(\Gamma_1 + \gamma_2) + \frac{1}{2}i(\Omega_1 + \omega_2) \mp \frac{1}{8}u, \quad u = \sqrt{4[(\Gamma_1 - \gamma_2) + 2i(\Omega_1 - \omega_2)]^2 - 64\eta_0^2}. \quad (\text{B12})$$

Under the parameter condition $\omega_{1,2} \gg \kappa \gg \tilde{G} \gg \{\Gamma_1, \gamma_{\text{opt}}\} \gg \gamma_{1,2}$, we have $\omega_1 \gg \omega_{\text{opt}}$. In the case of $\omega_1 = \omega_2 = \omega_m$, Eqs. (B10) and (B11) can then be reduced to the results in Eqs. (17).

-
- [1] T. J. Kippenberg and K. J. Vahala, Cavity optomechanics: Back-action at the mesoscale, *Science* **321**, 1172 (2008).
- [2] P. Meystre, A short walk through quantum optomechanics, *Ann. Phys. (Berlin)* **525**, 215 (2013).
- [3] M. Aspelmeyer, T. J. Kippenberg, and F. Marquardt, Cavity optomechanics, *Rev. Mod. Phys.* **86**, 1391 (2014).
- [4] P. Rabl, Photon Blockade Effect in Optomechanical Systems, *Phys. Rev. Lett.* **107**, 063601 (2011).
- [5] A. Nunnenkamp, K. Børkje, and S. M. Girvin, Single-Photon Optomechanics, *Phys. Rev. Lett.* **107**, 063602 (2011).
- [6] J.-Q. Liao, H. K. Cheung, and C. K. Law, Spectrum of single-photon emission and scattering in cavity optomechanics, *Phys. Rev. A* **85**, 025803 (2012).
- [7] A. Kronwald, M. Ludwig, and F. Marquardt, Full photon statistics of a light beam transmitted through an optomechanical system, *Phys. Rev. A* **87**, 013847 (2013).
- [8] J.-Q. Liao and C. K. Law, Correlated two-photon scattering in cavity optomechanics, *Phys. Rev. A* **87**, 043809 (2013).
- [9] J.-Q. Liao and F. Nori, Photon blockade in quadratically coupled optomechanical systems, *Phys. Rev. A* **88**, 023853 (2013).
- [10] X.-W. Xu, Y.-J. Li, and Y.-X. Liu, Photon-induced tunneling in optomechanical systems, *Phys. Rev. A* **87**, 025803 (2013).
- [11] G. S. Agarwal and S. Huang, The electromagnetically induced transparency in mechanical effects of light, *Phys. Rev. A* **81**, 041803 (2010).
- [12] B. P. Hou, L. F. Wei, and S. J. Wang, Optomechanically induced transparency and absorption in hybridized optomechanical systems, *Phys. Rev. A* **92**, 033829 (2015).
- [13] M. Bhattacharya and P. Meystre, Multiple membrane cavity optomechanics, *Phys. Rev. A* **78**, 041801(R) (2008).
- [14] A. Xuereb, C. Genes, and A. Dantan, Strong Coupling and Long-Range Collective Interactions in Optomechanical Arrays, *Phys. Rev. Lett.* **109**, 223601 (2012).
- [15] B. Nair, A. Xuereb, and A. Dantan, Cavity optomechanics with arrays of thick dielectric membranes, *Phys. Rev. A* **94**, 053812 (2016).
- [16] N. Spethmann, J. Kohler, S. Schreppler, L. Buchmann, and D. M. Stamper-Kurn, Cavity-mediated coupling of mechanical oscillators limited by quantum back-action, *Nat. Phys.* **12**, 27 (2016).
- [17] F. Massel, Mechanical entanglement detection in an optomechanical system, *Phys. Rev. A* **95**, 063816 (2017).
- [18] E. Gil-Santos, M. Labousse, C. Baker, A. Goetschy, W. Hease, C. Gomez, A. Lemaître, G. Leo, C. Ciuti, and I. Favero, Light-Mediated Cascaded Locking of Multiple Nano-Optomechanical Oscillators, *Phys. Rev. Lett.* **118**, 063605 (2017).
- [19] J. P. Paz and A. J. Roncaglia, Dynamics of the Entanglement between Two Oscillators in the Same Environment, *Phys. Rev. Lett.* **100**, 220401 (2008).
- [20] X.-W. Xu, Y.-J. Zhao, and Y.-X. Liu, Entangled-state engineering of vibrational modes in a multimembrane optomechanical system, *Phys. Rev. A* **88**, 022325 (2013).
- [21] Y.-D. Wang and A. A. Clerk, Reservoir-Engineered Entanglement in Optomechanical Systems, *Phys. Rev. Lett.* **110**, 253601 (2013).
- [22] J.-Q. Liao, Q.-Q. Wu, and F. Nori, Entangling two macroscopic mechanical mirrors in a two-cavity optomechanical system, *Phys. Rev. A* **89**, 014302 (2014).
- [23] M. J. Woolley and A. A. Clerk, Two-mode squeezed states in cavity optomechanics via engineering of a single reservoir, *Phys. Rev. A* **89**, 063805 (2014).
- [24] M. Wang, X.-Y. Lü, Y.-D. Wang, J. Q. You, and Y. Wu, Macroscopic quantum entanglement in modulated optomechanics, *Phys. Rev. A* **94**, 053807 (2016).
- [25] E. Damskägg, J.-M. Pirkkalainen, and M. A. Sillanpää, Dynamically creating tripartite resonance and dark modes in a multimode optomechanical system, *J. Opt.* **18**, 104003 (2016).
- [26] C. F. Ockeloen-Korppi, E. E. Damskägg, J.-M. Pirkkalainen, A. A. Clerk, F. Massel, M. J. Woolley, and M. A. Sillanpää, Stabilized entanglement of massive mechanical oscillators, *Nature (London)* **556**, 478 (2018).
- [27] A. Mari, A. Farace, N. Didier, V. Giovannetti, and R. Fazio, Measures of Quantum Synchronization in Continuous Variable Systems, *Phys. Rev. Lett.* **111**, 103605 (2013).
- [28] M. H. Matheny, M. Grau, L. G. Villanueva, R. B. Karabalin, M. C. Cross, and M. L. Roukes, Phase Synchronization of Two Anharmonic Nanomechanical Oscillators, *Phys. Rev. Lett.* **112**, 014101 (2014).
- [29] P. A. Truitt, J. B. Hertzberg, C. C. Huang, K. L. Ekinci, and K. C. Schwab, Efficient and sensitive capacitive readout of nanomechanical resonator arrays, *Nano Lett.* **7**, 120 (2007).
- [30] I. Bargatin, E. B. Myers, J. S. Aldridge, C. Marcoux, P. Brianceau, L. Duraffourg, E. Colinet, S. Hentz, P. Andreucci, and M. L. Roukes, Large-scale integration of nanoelectromechanical systems for gas sensing applications, *Nano Lett.* **12**, 1269 (2012).
- [31] H. Okamoto, A. Gourgout, C. Y. Chang, K. Onomitsu, I. Mahboob, E. Y. Chang, and H. Yamaguchi, Coherent phonon

- manipulation in coupled mechanical resonators, *Nat. Phys.* **9**, 480 (2013).
- [32] P. Huang, P. Wang, J. Zhou, Z. Wang, C. Ju, Z. Wang, Y. Shen, C. Duan, and J. Du, Demonstration of Motion Transduction Based on Parametrically Coupled Mechanical Resonators, *Phys. Rev. Lett.* **110**, 227202 (2013).
- [33] P. Huang, L. Zhang, J. Zhou, T. Tian, P. Yin, C. Duan, and J. Du, Nonreciprocal Radio Frequency Transduction in a Parametric Mechanical Artificial Lattice, *Phys. Rev. Lett.* **117**, 017701 (2016).
- [34] S. Mancini, D. Vitali, and P. Tombesi, Optomechanical Cooling of a Macroscopic Oscillator by Homodyne Feedback, *Phys. Rev. Lett.* **80**, 688 (1998).
- [35] P. F. Cohadon, A. Heidmann, and M. Pinard, Cooling of a Mirror by Radiation Pressure, *Phys. Rev. Lett.* **83**, 3174 (1999).
- [36] D. Kleckner and D. Bouwmeester, Sub-kelvin optical cooling of a micromechanical resonator, *Nature (London)* **444**, 75 (2006).
- [37] T. Corbitt, C. Wipf, T. Bodiya, D. Ottaway, D. Sigg, N. Smith, S. Whitcomb, and N. Mavalvala, Optical Dilution and Feedback Cooling of a Gram-Scale Oscillator to 6.9 mK, *Phys. Rev. Lett.* **99**, 160801 (2007).
- [38] M. Poggio, C. L. Degen, H. J. Mamin, and D. Rugar, Feedback Cooling of a Cantilever's Fundamental Mode below 5 mK, *Phys. Rev. Lett.* **99**, 017201 (2007).
- [39] A. Schliesser, P. Del'Haye, N. Nooshi, K. J. Vahala, and T. J. Kippenberg, Radiation Pressure Cooling of a Micromechanical Oscillator Using Dynamical Backaction, *Phys. Rev. Lett.* **97**, 243905 (2006).
- [40] R. W. Peterson, T. P. Purdy, N. S. Kampel, R. W. Andrews, P.-L. Yu, K. W. Lehnert, and C. A. Regal, Laser Cooling of a Micromechanical Membrane to the Quantum Backaction Limit, *Phys. Rev. Lett.* **116**, 063601 (2016).
- [41] I. Wilson-Rae, N. Nooshi, W. Zwerger, and T. J. Kippenberg, Theory of Ground State Cooling of a Mechanical Oscillator Using Dynamical Backaction, *Phys. Rev. Lett.* **99**, 093901 (2007).
- [42] F. Marquardt, J. P. Chen, A. A. Clerk, and S. M. Girvin, Quantum Theory of Cavity-Assisted Sideband Cooling of Mechanical Motion, *Phys. Rev. Lett.* **99**, 093902 (2007).
- [43] F. Xue, Y.-D. Wang, Y.-X. Liu, and F. Nori, Cooling a micromechanical beam by coupling it to a transmission line, *Phys. Rev. B* **76**, 205302 (2007).
- [44] K. R. Brown, J. Britton, R. J. Epstein, J. Chiaverini, D. Leibfried, and D. J. Wineland, Passive Cooling of a Micromechanical Oscillator with a Resonant Electric Circuit, *Phys. Rev. Lett.* **99**, 137205 (2007).
- [45] C. Genes, D. Vitali, P. Tombesi, S. Gigan, and M. Aspelmeyer, Ground-state cooling of a micromechanical oscillator: Comparing cold damping and cavity-assisted cooling schemes, *Phys. Rev. A* **77**, 033804 (2008); Erratum: Ground-state cooling of a micromechanical oscillator: Comparing cold damping and cavity-assisted cooling schemes [*Phys. Rev. A* **77**, 033804 (2008)], **79**, 039903(E) (2009).
- [46] Y. Li, Y.-D. Wang, F. Xue, and C. Bruder, Quantum theory of transmission line resonator-assisted cooling of a micromechanical resonator, *Phys. Rev. B* **78**, 134301 (2008).
- [47] Y. Li, L.-A. Wu, and Z. D. Wang, Fast ground-state cooling of mechanical resonators with time-dependent optical cavities, *Phys. Rev. A* **83**, 043804 (2011).
- [48] Y.-L. Liu and Y.-X. Liu, Energy-localization-enhanced ground-state cooling of a mechanical resonator from room temperature in optomechanics using a gain cavity, *Phys. Rev. A* **96**, 023812 (2017).
- [49] X. Xu, T. Purdy, and J. M. Taylor, Cooling a Harmonic Oscillator by Optomechanical Modification of Its Bath, *Phys. Rev. Lett.* **118**, 223602 (2017).
- [50] J.-Q. Liao and C. K. Law, Cooling of a mirror in cavity optomechanics with a chirped pulse, *Phys. Rev. A* **84**, 053838 (2011).
- [51] S. Machnes, J. Cerrillo, M. Aspelmeyer, W. Wieczorek, M. B. Plenio, and A. Retzker, Pulsed Laser Cooling for Cavity Optomechanical Resonators, *Phys. Rev. Lett.* **108**, 153601 (2012).
- [52] K. Xia and J. Evers, Ground State Cooling of a Nanomechanical Resonator in the Nonresolved Regime via Quantum Interference, *Phys. Rev. Lett.* **103**, 227203 (2009).
- [53] X.-T. Wang, S. Vinjanampathy, F. W. Strauch, and K. Jacobs, Ultraefficient Cooling of Resonators: Beating Sideband Cooling with Quantum Control, *Phys. Rev. Lett.* **107**, 177204 (2011).
- [54] Y. Li, L.-A. Wu, Y.-D. Wang, and L.-P. Yang, Nondeterministic ultrafast ground-state cooling of a mechanical resonator, *Phys. Rev. B* **84**, 094502 (2011).
- [55] L.-L. Yan, J.-Q. Zhang, S. Zhang, and M. Feng, Efficient cooling of quantized vibrations using a four-level configuration, *Phys. Rev. A* **94**, 063419 (2016).
- [56] Y.-C. Liu, Y.-F. Xiao, X. Luan, and C. W. Wong, Dynamic Dissipative Cooling of a Mechanical Resonator in Strong Coupling Optomechanics, *Phys. Rev. Lett.* **110**, 153606 (2013).
- [57] Y.-C. Liu, Y.-F. Shen, Q. Gong, and Y.-F. Xiao, Optimal limits of cavity optomechanical cooling in the strong-coupling regime, *Phys. Rev. A* **89**, 053821 (2014).
- [58] J. Chan, T. P. Alegre, A. H. Safavi-Naeini, J. T. Hill, A. Krause, S. Groeblacher, M. Aspelmeyer, and O. Painter, Laser cooling of a nanomechanical oscillator into its quantum ground state, *Nature (London)* **478**, 89 (2011).
- [59] J. D. Teufel, T. Donner, D. Li, J. W. Harlow, M. S. Allman, K. Cicak, A. J. Sirois, J. D. Whittaker, K. W. Lehnert, and R. W. Simmonds, Sideband cooling of micromechanical motion to the quantum ground state, *Nature (London)* **475**, 359 (2011).
- [60] C. Genes, D. Vitali, and P. Tombesi, Simultaneous cooling and entanglement of mechanical modes of a micromirror in an optical cavity, *New J. Phys.* **10**, 095009 (2008).
- [61] M. Karuza, C. Molinelli, M. Galassi, C. Biancofiore, R. Natali, P. Tombesi, G. Di Giuseppe, and D. Vitali, Optomechanical sideband cooling of a thin membrane within a cavity, *New J. Phys.* **14**, 095015 (2012).
- [62] N. Kralj, M. Rossi, S. Zippilli, R. Natali, A. Borrielli, G. Pandraud, E. Serra, G. Di Giuseppe, and D. Vitali, Enhancement of three-mode optomechanical interaction by feedback-controlled light, *Quantum Sci. Technol.* **2**, 034014 (2017).
- [63] L. Tian and P. Zoller, Coupled Ion-Nanomechanical Systems, *Phys. Rev. Lett.* **93**, 266403 (2004).
- [64] S. Schmid, L. G. Villanueva, and M. L. Roukes, *Fundamentals of Nanomechanical Resonators* (Springer, Switzerland, 2016).
- [65] I. S. Gradshteyn and I. M. Ryzhik, *Table of Integrals, Series, and Products* (Academic, New York, 2014).